

**MOF modified pencil electrode for hydrogen peroxide detections**Mostafa H. Fytory<sup>1</sup>, Soha M. Hamdy<sup>1</sup>, A. A. Farghali<sup>2</sup>, Roland Ludwig<sup>3</sup> and M.R. Saber<sup>1\*</sup><sup>1</sup> Chemistry department, Faculty of Sciences, Fayoum University, Fayoum, Egypt<sup>2</sup> Materials science and nanotechnology department, Faculty of postgraduate studies for advanced sciences, Beni-suef university, Beni-suef, Egypt.<sup>3</sup> Department of Food Science and Technology BOKU – University of Natural Resources and Life Sciences, Muthgasse 18, 1190 Vienna, Austria.**ARTICLE INFO****Keywords:***Pencil graphite electrode (PGE), MOF biosensors, H<sub>2</sub>O<sub>2</sub> detection, CDH, Pt electrode.***Abbreviations***MOF, Metal organic frame work  
CDH, Cellobiose dehydrogenase  
PGE, Pencil graphite electrode  
LOD, Limit of detection***ABSTRACT**

**Background:** Hydrogen peroxide is a key component of fungal biomass degradation. Fungal extracellular enzymes can produce this reactive oxygen species or depend on it as a co-substrate. The measurement of H<sub>2</sub>O<sub>2</sub> in proximity of enzymes bound to biomass is important to elucidate its production rate by oxidases, its consumption rate by peroxidases. **Objectives** This work reports the fabrication and characterization of pencil graphite electrode (PGE) and its application to measure the H<sub>2</sub>O<sub>2</sub> production by cellobiose dehydrogenase (CDH). **Methods:** The limit of detection (LOD) and the sensitivity of pencil graphite electrode were detected for both of bare and modified PGE, respectively. The H<sub>2</sub>O<sub>2</sub> generation of cellulose immobilized CDH was measured using the MOF modified PGE. CDH produces H<sub>2</sub>O<sub>2</sub> in the presence of cellobiose as a substrate. **Results:** MOF modified PGE exhibited low LODs (571 μM) and high sensitivities (2.35 μA mM<sup>-1</sup>mm<sup>-1</sup>). The lower acquisition costs and higher simplicity compensate for the higher LODs and lower sensitivities when compared to platinum electrodes. **Conclusions:** PGE was easy to fabricate, multiply usable and cost effective which make it a strong and promising tool for H<sub>2</sub>O<sub>2</sub> measuring.

**INTRODUCTION:**

H<sub>2</sub>O<sub>2</sub> is considered the most common reactive oxygen species (ROS) and by-product of the oxidative metabolic pathway (Lu, Wen, and Li 2006). Simple and reliable hydrogen peroxide (H<sub>2</sub>O<sub>2</sub>) measurements are needed in different fields in recent years, because of the important role of H<sub>2</sub>O<sub>2</sub> in chemicals production, fuel cells, biotechnology, environmental, pharmaceutical and clinical applications (Jia et al. 2014; Reza and Bagheri 2014; Sawangphruk et al. 2014;

Tang, Yuan, and Chai 2006; Toniolo et al. 2011).

Many approaches were introduced to detect H<sub>2</sub>O<sub>2</sub> including chromatography (Toyo, Kashiwazaki, and Kato 2003), spectrometry (Matsubara, Kawamoto, and Takamura 1992), fluorescence, chemiluminescence (Taylor et al. 2006) and titrimetry (Hurdis and Romeyn 1954). Among all techniques, electrochemical methods in H<sub>2</sub>O<sub>2</sub> detection are still the affordable choice due to their advantages (low cost, fast response and high

Corresponding Author: Dr. Mohamed R. Saber, Ph.D.

Lecturer of chemistry & Materials sciences, Faculty of Sciences, Fayoum University  
University Street, Fayoum 63511, Egypt.

Telephone: +202 - 01006036739

Fax: +202 - 0846370025

E-mail: msaber@fayoum.edu.eg

sensitivity). Thus, many achievements in electrochemical detection of  $H_2O_2$  have been reported (Chemishy 1989; Guascito et al. 2008; Lvovich and Scheeline 1997; MasuoAizawa, IsaoKarube 1974; Wu et al. 2006), of which the enzymatic and nonenzymatic hydrogen peroxide electrochemical sensing are the most common techniques in  $H_2O_2$  detection (Zhenting Zhao, Qibiao Ou 2017).

Due to the high surface area and the porosity of MOF, many molecules could be loaded on it, which catalyze the target with a high catalytic activity that affords inherent sensitivity for the electrochemical detection. In the face of the enticing features of MOFs introduce them as an excellent material for electrode modification, still there are two challenges to be addressed: the design of redox active MOFs and the improvement on MOF conductivity (Pauliukaite et al. 2008). Moreover, because of their high surface areas, naked active sites, specific adsorption affinity and various pore sizes MOFs were used for electrode surface modification in order to detect trace amounts of compounds (Dong et al. 2016; Kung et al. 2015; Li et al. 2013; X. Wang et al. 2015; D. Zhang et al. 2015).

Due to the wide potential window, chemical inertness and low cost, carbon-based materials have been considered as an important electrode material for electrochemical biosensors. Different carbon allotropes have been used for biosensor fabrication for the detection of  $H_2O_2$ . Among the carbon-based electrodes, pencil graphite electrodes (PGE), glassy carbon electrodes (GCE) and carbon fiber electrodes (CFE) are three of the most widely used electrodes. Pencil graphite electrodes (PGEs) are carbon-based electrodes that are identified by their cost-effectiveness, simplicity, commercial availability, high surface area, and high conductivity. PGEs are attractive materials for electrochemical sensing owing to their exclusive feature of "disposability" compared to other commonly used carbon-

based electrodes (A.-N. Kawde, Baig, and Sajid 2016). In addition, PGEs are mechanically rigid and easy to modify and miniaturize (David, Badea, and Radu 2013). Modification of PGE with nanomaterials or direct formation of NPs on PGE surface enhances its surface area, which in turn results in high sensitivity and improved electrochemical activity towards the detection of target species (A.-N. Kawde, Baig, and Sajid 2016). A variety of nanomaterials have been applied for modifications of PGE such as metal nanoparticles (Aziz and Kawde 2013a), conducting polymers, carbon-based materials (Kuralay, Dumangöz, and Tunç 2015). Due to high selectivity and sensitivity, portability, rapid analysis, and ease of availability, modified PGEs offer excellent opportunities for detections of many environmental and biological samples (Alipour, Reza, and Saadatirad 2013; Rezaei 2014; Tadi, Motghare, and Ganesh 2014). Moreover as reported very recently, modified PGEs show a high electrocatalytic activity toward  $H_2O_2$  detection. (Aziz and Kawde 2013b; A. Kawde, Baig, and Temerk 2015; J. Zhang and Zheng 2015). Herein, sensors using pencil graphite were fabricated through a very simple process and modified with UiO-66 MOF. In addition, design, fabrication, and operation of a 2D scanning electrochemical micro-copy cell for the amperometric detection of enzymatically produced  $H_2O_2$ .

## **MATERIALS AND METHODS:**

### **Materials and enzymes**

The MDA-MB-231 cell line, known as a wild-type for BRCA human triple-negative breast cancer cell line, was obtained from Vacsera (Dokki, Giza, Egypt) and processed in National Cancer Institute, Cairo University. The MDA-MB-231 cells were cultured in DMEM medium (Sigma, St Louis, MO, USA) containing 10% fetal bovine serum along with 100 mg/ml streptomycin and 100 units/ml penicillin G (Sigma, St Louis, MO, USA). Cells were incubated in a

humidified atmosphere with 5% (v/v) CO<sub>2</sub> at 37°C. For drug treatment, 10mg of olaparib (LKT Laboratories, USA) was dissolved in 1ml DMSO and stored at -4°C upon usage.

#### **CDH assay using cytochrome c and DCIP**

CDH activity was measured based on monitoring the reduction of 20 μM cytochrome c (cyt c) ( $\epsilon_{550} = 19.6 \text{ mM}^{-1} \text{ cm}^{-1}$ ) or 0.3 mM 2,6-dichlorophenolindophenol (DCIP) ( $\epsilon_{520} = 6.8 \text{ mM}^{-1} \text{ cm}^{-1}$ ). 100 μL of the electron acceptor solution and 100 μL lactose solution (30 mM in distilled water) was added to 780 μL 100 mM phosphate buffer, pH 6.0. Cuvettes were incubated in a water bath at 30°C for 20 min. The reaction was monitored at 550 or 520 nm for 3 min at 30°C in a Lambda 35 UV-visible (UV-Vis) spectrophotom.

#### **Fabrication of MOF modified Pencil Graphite Electrode (PGE).**

All leads with a diameter of 0.5 mm were used as received. A copper wire was soldered to the pencil leads for electrical contact. Contacted leads of ~ 1 cm length were put into standard borosilicate glass capillaries with filament (OD 1.50 mm, ID 0.86 mm, Sutter Instrument, Novato, CA, USA) leaving out ~ 1 mm at one side of the capillary. At this side, the nozzle, including the salient part of the lead, was sealed using graphite conductive adhesive 154 (Electron Microscopy Sciences). The sealed leads were then polished using wet emery paper (P400 and P2500) until they were in the plane with the surrounding glass capillary. The electrode was then rinsed with distilled water and dried at room temperature overnight. PGE microelectrode were modified with simple way. A solution of 1.5 mg ml<sup>-1</sup> UiO-66(Zr) MOF in HQ-H<sub>2</sub>O was prepared by sonicating for 15 min. The prepared electrodes were immersed in a 3mL tube containing 1 ml of the synthesized UiO-66 (Zr) MOF and sonicated for 30 min at room temperature. The UiO-66(Zr) modified electrodes were then washed

gently with distilled water and dried at room temperature before use.

#### **Electrochemical Measurements.**

All electrochemical measurements were performed with a standard three-electrode setup employing an Ag/AgCl-reference electrode (3 M KCl), a platinum wire as a counter electrode and a pencil electrode as a working electrode using a PGSTAT204 Potentiostat/Galvanostat (Metrohm Autolab, Utrecht, The Netherlands). Calibration curves were obtained by using chronoamperometry applying a potential of -0.4 V vs Ag/AgCl (3 M KCl) adding aliquots of H<sub>2</sub>O<sub>2</sub> to 50 mL stirred KPP buffer solution, pH 6.0, at defined time intervals and plotting the current I versus the respective H<sub>2</sub>O<sub>2</sub> concentrations.

#### **RESULTS:**

##### **Characterization of UiO-66 and modification of carbon electrodes.**

The Zr-based MOF UiO-66 was synthesized as mentioned above in materials and methods section. The resulting white powder was collected and the crystal structure of the prepared UiO-66 MOF was examined using Powder X-ray diffraction (PXRD). XRD pattern, FTIR spectra and FE SEM of the synthesized UiO-66 MOF is shown in (Figure 1a, b and 2).

##### **Fabrication of MOF modified Pencil Graphite Electrodes (PGEs)**

Briefly, (PGEs) as a sensor were simply designed by connecting graphite pencil (0.5 mm diameter, 2mm length) with copper wire as an electrical conductor in glass capillary. A PGE was immersed in the synthesized UiO-66 MOF solution for 15 min at room temperature. After washing and drying, chronoamperometry was applied in 50 mM of KPP pH 6.0 for both bare PGE and modified electrode.

##### **Amperometric response of working electrode.**

The amperometric responses of the bare and MOF modified Pencil Graphite Electrodes (PGEs) microelectrodes in

comparison with platinum microelectrode were measured by successive injections of different concentrations of  $\text{H}_2\text{O}_2$  in 50 mM KPP (pH 6.0) under stirring at an applied potential of -0.4 V with a time interval of 60 s as indicated in Fig 3. (**Figure 3a**) shows the stable amperometric response of Pt microelectrode with a 25  $\mu\text{M}$  diameter. The steady-state current was obtained after a very reasonable time (2 second) of additions of  $\text{H}_2\text{O}_2$ . (**Figure 3b**) shows the amperometric responses of the bare PGE (solid red line) UIO-66 modified PGE (solid black line) at -0.4V upon successive additions of  $\text{H}_2\text{O}_2$  with interval time 30 s. The UIO-66 modified PGE (**Fig. 3b black**) offered a very well-defined and sensitive signal for each addition of  $\text{H}_2\text{O}_2$ , in comparison with the bare PGE (**Figure. 3b red**) that showed a weak signal.

#### **Calibration curve of working electrodes, determination of LOD and sensitivity.**

A calibration curve observed at the different types of microelectrode was undertaken to assess the potential impact of MOF modifications on microelectrode. **Figure 4** shows the calibration data for the different types of microelectrodes over the range of 0.25- 5.0 mM  $\text{H}_2\text{O}_2$ . For a Pt microelectrode (25 $\mu\text{m}$  in diameter) the active surface area of Pt, assuming a disk-shaped surface, was calculated according to  $A = \pi r^2 = 0.000490874 \text{ mm}^2$ . The quality of the calibration data obtained for the Pt microelectrode is remarkable. A linear response is observed for the Pt microelectrode. Weighted regression of the data ( $R^2 = 0.996$ ) over the range of 0.25-5.0 mM yields a sensitivity of the Pt microelectrode calculated from the slope of the calibration plot between 0.25 and 5 mM of  $4.16 \mu\text{A mM}^{-1} \text{ mm}^{-2}$ . The limit of detection (LOD), considered as the limiting current for  $\text{H}_2\text{O}_2$  detection and measured as 3 times the standard deviation of the blank divided by sensitivity was found to be 200.45  $\mu\text{M}$ . The Limit of quantification (LOQ), was calculated as 10 times the standard deviation of the blank divided by sensitivity was found to be

668.12  $\mu\text{M}$ . The surface area of a graphite pencil electrode (0.5 mm in diameter), assuming a disk-shaped surface, was calculated according to  $A = (\pi r^2) = 0.1964 \text{ mm}^2$ . Figure 4b shows the electrocatalytic activity of bare PGE and the UIO-66/GPE for amperometric detection of  $\text{H}_2\text{O}_2$  at an operating potential of -0.4V upon successive additions of 0.25, 0.5, 0.75, 1, 2, 3, 4, and 5 mM  $\text{H}_2\text{O}_2$ . Weighted regression of the data for the UIO-66/GPE and the bare PGE ( $R^2 = 0.996$  and  $0.995$ , respectively) over the range of 0.25-5 mM yielded in a sensitivity of  $2.16 \mu\text{A mM}^{-1} \text{ mm}^{-2}$  and  $0.751 \mu\text{A mM}^{-1} \text{ mm}^{-2}$ , respectively. The LODs were 610 and 0.214  $\mu\text{M}$ , respectively. The LOQs were 2070 and 803  $\mu\text{M}$ , respectively. A comparison of the limit of detection, the linear range and the sensitivity of the here prepared microelectrodes with MOFs modified  $\text{H}_2\text{O}_2$  sensors from the literature are given in (**Table 1**).

#### **2D-scanning electrochemical microscopy for measuring $\text{H}_2\text{O}_2$ as a by-product of enzymatic reactions.**

The SECM set-up used in the electrochemical enzymatic reaction measurements was described previously in published work(Sun 2012). The main components of a SECM set-up are the micromanipulator used for positioning of the SECM tip in x-, y-, and z- direction, a potentiostat, a computer and an ultramicroelectrode. Here, we used MOF modified carbon electrodes as SECM tips in the homemade electrochemical cell. All SECM measurements were performed in 50 mM KPP, pH 6.0. A buffered solution has been chosen to be suitable with the enzyme conditions used in the measurements. Experiments were carried out applying a standard three-electrode setup comprising a Ag/AgCl (3M KCl) silverchloride electrode was used as a reference electrode, a Pt wire as a counter electrode and MOF modified and unmodified pencil as working electrode. A cellulose filter paper was used as the basis

for protein immobilization. Fig 5 schematically illustrates the enzymatic reaction occurring in the electrochemical cell. It shows that CDH catalyzes the oxidation of cellobiose to cellobionic acid followed by the reduction of  $\text{H}_2\text{O}_2$  to  $\text{O}_2$ .

#### **MOF/Pencil electrode as amperometric sensor for the detection of $\text{H}_2\text{O}_2$ produced from CDH immobilized on cellulose.**

The collected amperometric response is proportional to the concentration of the present  $\text{H}_2\text{O}_2$ . With the help of the respective calibration curves, the actual concentration of  $\text{H}_2\text{O}_2$  was calculated. For the SECM experiments we defined and kept constant a specific scan rate for the forward and backward scans ( $\mu\text{m s}^{-1}$ ). Thus, we were able to convert the raw data from the chronoamperometric experiments (current and time) to concentrations of  $\text{H}_2\text{O}_2$  and distance. Plotting of these variables reveals a spatial resolution of  $\text{H}_2\text{O}_2$  concentrations in the bulk solution and is shown in (Figure 6) for the tested electrode.

#### **DISCUSSION:**

The structure of the synthesized sample is confirmed by the good agreement between the XRD patterns of the sample and the simulated pattern. FTIR spectra of the MOF sample were collected in the range of  $4000\text{--}400\text{ cm}^{-1}$  as KBr pellets (Figure 1b). The stretching vibration and bending vibration bands around  $1607$  and  $1408\text{ cm}^{-1}$  are attributed to  $\nu_{\text{as}}(\text{COO})$  and  $\nu_{\text{s}}(\text{COO})$  which confirms the presence of terephthalate ligands. The band centered at  $3391\text{ cm}^{-1}$  in the frequency region between ( $3800\text{--}3100\text{ cm}^{-1}$ ) can be assigned to the hydrogen-bonded adsorbed water and  $\nu(\text{C-H})$  stretching modes of DMF molecules. The aromatic and aliphatic  $\nu(\text{C-H})$  modes of the benzene ring and DMF are indicated by the presence of the weak bands in the  $3100\text{--}2850\text{ cm}^{-1}$  region. The low frequency region is dominated by an intense band centered at  $1658\text{ cm}^{-1}$  and two narrow

bands at  $1255$  and  $1102\text{ cm}^{-1}$ . These bands could be assigned to the  $\delta(\text{OH}_2)$ ,  $\delta(\text{CH}_3)$  and  $\delta(\text{C-O})$  vibration of the physisorbed water and DMF molecules, respectively. The morphological structure of the pristine sample was examined using FE-SEM at different magnification scales ( $2\mu\text{m}$  and  $5\mu\text{m}$ ). As shown in Fig 2. 1c, 2c, and 3c, the prepared UiO-66 appears as relatively uniform particles with a particle size in the nanoscale range ( $100\text{--}200\text{ nm}$ ).

Fig 3a shows the stable amperometric response of Pt microelectrode with a  $25\text{ }\mu\text{m}$  diameter. The steady-state current was obtained after a very reasonable time (2 second) of additions of  $\text{H}_2\text{O}_2$ . Fig 3b shows the amperometric responses of the bare PGE (solid red line) UIO-66 modified PGE (solid black line) at  $-0.4\text{V}$  upon successive additions of  $\text{H}_2\text{O}_2$  with interval time  $30\text{ s}$ . The UIO-66 modified PGE (Fig. 3b black) offered a very well-defined and sensitive signal for each addition of  $\text{H}_2\text{O}_2$ , in comparison with the bare PGE (Fig. 3b red) that showed a weak signal. This is a direct effect of the MOF surface modifications on the electrocatalytic properties of the prepared electrode. The data from Fig 3b for both bare PGE and UIO-66/PGE confirmed that the bare PGE displayed poor electrocatalytic properties with respect to the reductions of  $\text{H}_2\text{O}_2$  compared to that observed for the UIO-66/PGE. The reduction of  $\text{H}_2\text{O}_2$  at the UIO-66/PGE could be attributed to the excellent electrocatalytic properties of the UIO-66 MOF. Moreover, the UIO-66 MOF played as suitable mediators to shuttle electrons between  $\text{H}_2\text{O}_2$  and PGE, and they facilitated the electrochemical generation following electron exchange with  $\text{H}_2\text{O}_2$ .

The accuracy of the data is very reasonable, which make Pt microelectrode sensor able to quantitatively measure  $\text{H}_2\text{O}_2$  amperometrically. This fact gives a suggestion for the potential use of Pt microelectrode in a wide range of applications from very low levels of

hydrogen peroxide produced in vivo due to oxidative cell stress to the millimolar levels presented in some industrial processes (Amatore et al. 2000). Moreover, the range of linearity offered covers more than that obtained by field strips common in commercial use (Evans et al. 2002).

With UIO-66 modification, the sensitivity of a pencil graphite electrode could thus be improved by almost a factor of four. The high sensitivity of modified electrode comes from the fact that MOF on the surface of PGE increases the surface area of the electrode, therefore, increases the electrocatalytic performance of the electrode towards  $H_2O_2$  reduction. The above discussion indicates that UIO-66 - PGE offers higher electrocatalytic properties towards the detection of  $H_2O_2$  in comparison with the bare PGE. A comparison of the limit of detection, the linear range and the sensitivity of the here prepared microelectrodes with MOFs modified  $H_2O_2$  sensors from the literature are given in Table 1. Based on this comparative study, it was found that the UIO-66/carbon electrodes can offer affordable LOD and high sensitivity for the detection of  $H_2O_2$ .

Recently, new approaches were applied based on PGE for sensing of  $H_2O_2$  (A.-N. Kawde, Baig, and Sajid 2016). Modification of PGE with nanomaterials has aroused great attention in  $H_2O_2$  detection owing to its high sensitivity. For measuring  $H_2O_2$  produced from cellobiose dehydrogenase we used a UIO-66 MOF modified PGE. A very fine drop of CDH enzyme was immobilized on the middle of a cellulose paper with a length of 2.5 cm fixed on the bottom of the homemade electrochemical cell. The cell was filled with 50 mM KPP, pH 6.0, serving both as buffer solution and electrolyte, and 10 mM cellobiose solution serving as a substrate for CDH. UIO-66/PGE was used as SECM tip. The measurement started by moving UIO-

66/PGE above the immobilized enzyme in the electrochemical cell using the micromanipulator. The electrode was then scanned successively forwards and backwards along the y-axis over the whole length of the cell, thereby screening over the immobilized  $H_2O_2$  producing (CDH) and  $H_2O_2$  consuming (CDH/LPMO) enzymes. The CDH catalyzed generated  $H_2O_2$  travels vertically out from the immobilized CDH in a hemispherical shape and is amperometrically detected with the positioned UIO-66/PGE tip at a very close distance to the immobilized CDH.

**Figure 6.** represents the data collected from the amperometric detection of  $H_2O_2$  at the applied potential of -0.4V using a MOF modified PGE as working electrode. The solid line represents the data collected from the 1<sup>st</sup> forward scan and the dotted line refers to the 2<sup>nd</sup> forward scan. The data show that in the beginning of 1<sup>st</sup> forward scan (far away from the immobilized enzyme) almost no change in current was observed. In close vicinity of the immobilized CDH the current starts to increase reaching a peak maximum, when the electrode tip is positioned above the enzyme. Continuing the scan and thus moving the electrode further away from the immobilized CDH, the current decreases and soon reaches its initial background level. The higher background current in the 2<sup>nd</sup> forward scan may be attributable to further diffusion of the generated  $H_2O_2$  into the bulk solution over the whole cell distance. The lower peak maximum in the 2<sup>nd</sup> forward scan simply results from a shorter, in terms of time, stop in scanning in order to reach a maximum current right above the enzyme (as was done in the 1<sup>st</sup> forward scan). From the data in **Figure 6** and the explanations mentioned above, we can conclude that a UIO-66 MOF modified PGE is a suitable detector for  $H_2O_2$  produced from cellobiose fueled CDH.

**CONCLUSION:**

The fabrication of a MOF modified pencil graphite microelectrode with high sensitivity to detect the enzymatic production and conversion of  $H_2O_2$  by cellulose bound enzymes and to determine the concentration and diffusion of  $H_2O_2$  were achieved. CDH produces  $H_2O_2$  in the presence of cellobiose as a substrate. Comparisons between Pt microelectrode and both of bare and modified pencil graphite electrode used for  $H_2O_2$  detections were done.

**ACKNOWLEDGEMENT:**

This work was funded European Union joint master program (TEMPUS). The authors would like to thank his supervision committee for their assistance, expert guidance, sustained interest, fruitful revising of this manuscript.

**REFERENCES:**

- Alipour, Esmaeel, Mir Reza, and Afsaneh Saadatirad. 2013. "Electrochimica Acta Simultaneous Determination of Dopamine and Uric Acid in Biological Samples on the Pretreated Pencil Graphite Electrode." *Electrochimica Acta* 91: 36–42.  
<http://dx.doi.org/10.1016/j.electacta.2012.12.079>.
- Amatore, C et al. 2000. "Analysis of Individual Biochemical Events Based on Artificial Synapses Using Ultramicroelectrodes: Cellular Oxidative Burst." *Faraday Discussions* 116: 319–33.
- Arul, P., and S. Abraham John. 2017. "Silver Nanoparticles Built-in Zinc Metal Organic Framework Modified Electrode for the Selective Non-Enzymatic Determination of  $H_2O_2$ ." *Electrochimica Acta* 235: 680–89.  
<http://dx.doi.org/10.1016/j.electacta.2017.03.097>.
- Aziz, Abdul, and Abdel-nasser Kawde. 2013a. "Gold Nanoparticle-Modified Graphite Pencil Electrode for the High-Sensitivity Detection of Hydrazine." *Talanta* 115: 214–21.  
<http://dx.doi.org/10.1016/j.talanta.2013.04.038>.
- 2013b. "Nanomolar Amperometric Sensing of Hydrogen Peroxide Using a Graphite Pencil Electrode Modified with Palladium Nanoparticles." *Microchim Acta* 843: 837–43.
- Chemistry, Analytical. 1989. "An Electrochemical Sensor for Hydrogen Peroxide Based on Peroxidase Adsorbed on a Spectrographic Graphite Electrode." *Electroanalysis* 1: 465–68.
- David, Iulia Gabriela, Irinel Adriana Badea, and Gabriel Lucian Radu. 2013. "Disposable Carbon Electrodes as an Alternative for the Direct Voltammetric Determination of Alkyl Phenols from Water Samples." *Turk J Chem* 37: 91–100.
- Dong, Sheying et al. 2016. "A Simple Strategy to Fabricate High Sensitive 2,4-Dichlorophenol Electrochemical Sensor Based on Metal Organic Framework  $Cu_3(BTC)_2$ ." *Sensors and Actuators, B: Chemical* 222: 972–79.  
<http://dx.doi.org/10.1016/j.snb.2015.09.035>.
- Evans, Stuart a G et al. 2002. "Detection of Hydrogen Peroxide at Mesoporous Platinum Microelectrodes." *Analytical Chemistry* 74(6): 1322–26.
- Guascito, M. R. et al. 2008. "A New Amperometric Nanostructured Sensor for the Analytical Determination of Hydrogen Peroxide." *Biosensors and*

- Bioelectronics 24(4): 1057–63.
- Hurdis, Everett C, and Hendrik Romeyn. 1954. "Accuracy of Determination of Hydrogen Peroxide by Cerate Oxidimetry." *Analytical Chemistry* 26: 320–25.
- Jia, Ningming et al. 2014. "A Simple Non-Enzymatic Hydrogen Peroxide Sensor Using Gold Nanoparticles-Graphene-Chitosan Modified Electrode." *Sensors and Actuators, B: Chemical* 195: 165–70. <http://dx.doi.org/10.1016/j.snb.2014.01.043>.
- Kawde, Abdel-Nasser, Nadeem Baig, and Muhammad Sajid. 2016. "Graphite Pencil Electrodes as Electrochemical Sensors for Environmental Analysis: A Review of Features, Developments, and Applications." *RSC Adv.* 6(94): 91325–40. <http://xlink.rsc.org/?DOI=C6RA17466C>.
- Kawde, Abdel-nasser, Nadeem Baig, and Yassin Temerk. 2015. "A Facile Fabrication of Platinum Nanoparticle-Modified Graphite Pencil Electrode for Highly Sensitive Detection of Hydrogen Peroxide." *JOURNAL OF ELECTROANALYTICAL CHEMISTRY* 740: 68–74. <http://dx.doi.org/10.1016/j.jelechem.2015.01.005>.
- Kung, Chung Wei et al. 2015. "Porphyrin-Based Metal-Organic Framework Thin Films for Electrochemical Nitrite Detection." *Electrochemistry Communications* 58: 51–56. <http://dx.doi.org/10.1016/j.elecom.2015.06.003>.
- Kuralay, Filiz, Mehmet Dumangöz, and Selma Tunç. 2015. "Carbon Nanotubes Coated Graphite Surfaces for Highly Sensitive Nitrite Detection." *Talanta* 144: 1133–38. <http://dx.doi.org/10.1016/j.talanta.2015.07.095>.
- Li, Yingwei et al. 2013. "Electrochemical Behavior of Metal-Organic Framework MIL-101 Modified Carbon Paste Electrode: An Excellent Candidate for Electroanalysis." *Journal of Electroanalytical Chemistry* 709: 65–69. <http://dx.doi.org/10.1016/j.jelechem.2013.09.017>.
- Lu, Xianbo, Zhenhai Wen, and Jinghong Li. 2006. "Hydroxyl-Containing Antimony Oxide Bromide Nanorods Combined with Chitosan for Biosensors." *Biomaterials* 27(33): 5740–47.
- Lvovich, Vadim, and Alexander Scheeline. 1997. "Amperometric Sensors for Simultaneous Superoxide and Hydrogen Peroxide Detection." *Anal.Chem.* 69(3): 3579–87.
- MasuoAizawa, IsaoKarube, ShuichiSuzuki. 1974. "A Specific Bio-Electrochemical Sensor for Hydrogen Peroxide." *Analytica Chimica Acta* 69: 431–37.
- Matsubara, Chiyo, Naoki Kawamoto, and Kiyoko Takamura. 1992. "An Ultra-High Sensitivity Spectrophotometric Reagent for Hydrogen Peroxide." 117(November): 1781–84.
- Pauliukaite, Rasa, Samo B. Hočevar, Emily A. Hutton, and Božidar Ogorevc. 2008. "Novel Electrochemical Microsensor for Hydrogen Peroxide Based on Iron-Ruthenium Hexacyanoferrate Modified Carbon Fiber Electrode." *Electroanalysis* 20(1): 47–53.
- Reza, Mohammad, and Akbar Bagheri.



2014. "Sensors and Actuators B: Chemical Nonenzymatic Glucose and Hydrogen Peroxide Sensors Based on Catalytic Properties of Palladium Nanoparticles / Poly ( 3 , 4-Ethylenedioxythiophene ) Nanofibers." *Sensors & Actuators: B. Chemical* 195: 85–91. <http://dx.doi.org/10.1016/j.snb.2014.01.015>.
- Rezaei, Heydari-bafrooei B. 2014. "Development of a Voltammetric Procedure Based on DNA Interaction for Sensitive Monitoring of Chrysoidine, a Banned Dye, in Foods and Textile Effluents." *Sensors & Actuators: B. Chemical* 202: 224–31. <http://dx.doi.org/10.1016/j.snb.2014.05.001>.
- Sawangphruk, Montree et al. 2014. "Silver Nanodendrite Modified Graphene Rotating Disk Electrode for Nonenzymatic Hydrogen Peroxide Detection." *Carbon* 70(0): 287–94. <http://dx.doi.org/10.1016/j.carbon.2014.01.010>.
- Sherino, Bibi, Sharifah Mohamad, Siti Nadiah Abdul Halim, and Ninie Suhana Abdul Manan. 2018. "Electrochemical Detection of Hydrogen Peroxide on a New Microporous Ni-metal Organic Framework Material-Carbon Paste Electrode." *Sensors and Actuators, B: Chemical* 254: 1148–56. <http://dx.doi.org/10.1016/j.snb.2017.08.002>.
- Sun, Yu. 2012. "Scanning Electrochemical Microscopy Studies of Nickel Surfaces and T24 Single Live Cells."
- Tadi, Kiran Kumar, R V Motghare, and V Ganesh. 2014. "Electrochemical Detection of Sulfanilamide Using Pencil Graphite Electrode Based on Molecular Imprinting Technology." *Electroanalysis* 26: 2328 – 2336.
- Tang, Dianping, Ruo Yuan, and Yaqin Chai. 2006. "Electron-Transfer Mediator Microbiosensor Fabrication Based on Immobilizing HRP-Labeled Au Colloids on Gold Electrode Surface by 11-Mercaptoundecanoic Acid Monolayer." *Electroanalysis* 18(3): 259–66.
- Taylor, Publisher, M Aizawa, Y Ikariyama, and H Kuno. 2006. "Photovoltaic Determination of Hydrogen Peroxide with A Biophotodiode." *Analytical Letters* 17(July 2015): 555–64.
- Toniolo, Rosanna et al. 2011. "Simultaneous Detection of Ascorbic Acid and Hydrogen Peroxide by Flow-Injection Analysis with a Thin Layer Dual-Electrode Detector." *Electroanalysis* 23(3): 628–36.
- Toyo, Toshimasa, Tomoaki Kashiwazaki, and Masaru Kato. 2003. "On-Line Screening Methods for Antioxidants Scavenging Superoxide Anion Radical and Hydrogen Peroxide by Liquid Chromatography with Indirect Chemiluminescence Detection." 60: 467–75.
- Wang, Li et al. 2016. "Cu-Hemin Metal-Organic-Frameworks/Chitosan-Reduced Graphene Oxide Nanocomposites with Peroxidase-Like Bioactivity for Electrochemical Sensing." *Electrochimica Acta* 213: 691–97. <http://dx.doi.org/10.1016/j.electacta.2016.07.162>.
- Wang, Xue, Xianbo Lu, Lidong Wu, and Jiping Chen. 2015. "3D Metal-Organic Framework as Highly Efficient Biosensing Platform for Ultrasensitive and Rapid Detection

- of Bisphenol A.” *Biosensors and Bioelectronics* 65: 295–301. <http://dx.doi.org/10.1016/j.bios.2014.10.010>.
- Wu, Shuo et al. 2006. “Electrodeposition of Silver – DNA Hybrid Nanoparticles for Electrochemical Sensing of Hydrogen Peroxide and Glucose.” *Electrochemistry Communications* 8: 1197–1203.
- Xu, Zhaodong, Lizi Yang, and Cailing Xu. 2015. “Pt@UiO-66 Heterostructures for Highly Selective Detection of Hydrogen Peroxide with an Extended Linear Range.” *Analytical Chemistry* 87(6): 3438–44.
- Yang, Lizi, Cailing Xu, Weichun Ye, and Weisheng Liu. 2015. “An Electrochemical Sensor for H<sub>2</sub>O<sub>2</sub> Based on a New Co-Metal-Organic Framework Modified Electrode.” *Sensors and Actuators, B: Chemical* 215: 489–96. <http://dx.doi.org/10.1016/j.snb.2015.03.104>.
- Zhang, Daojun et al. 2015. “3D Porous Metal-Organic Framework as an Efficient Electrochemical Sensor for Nonenzymatic Sensing Application.” *Talanta* 144: 1176–81. <http://dx.doi.org/10.1016/j.talanta.2015.07.091>.
- Zhang, Jian, and Jianbin Zheng. 2015. “Analytical Methods An Enzyme-Free Hydrogen Peroxide Sensor Based.” *Analytical Methods* 7: 1788–93. <http://dx.doi.org/10.1039/C4AY02881C>.
- Zhenting Zhao, Qibiao Ou, Xiuwen Yin and Jianqi Liu. 2017. “Nanomaterial-Based Electrochemical Hydrogen Peroxide Biosensor.” *International Journal of Biosensors & Bioelectronics* 2(3): 25–28.
- Zhou, Echeng, Yanwu Zhang, Yijun Li, and Xiwen He. 2014. “Cu(II)-Based MOF Immobilized on Multiwalled Carbon Nanotubes: Synthesis and Application for Nonenzymatic Detection of Hydrogen Peroxide with High Sensitivity.” *Electroanalysis* 26(11): 2526–33.

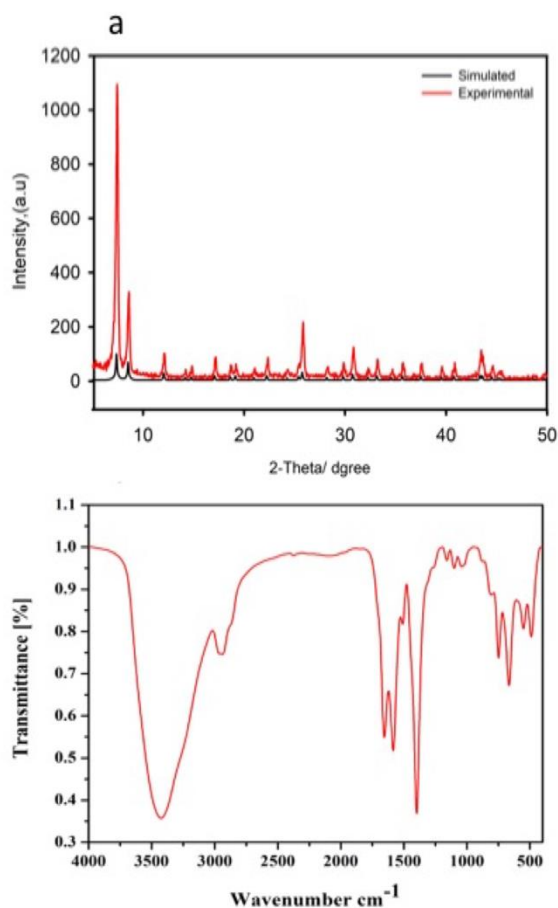


Figure (1): XRD patterns of prepared UIO-66 MOF and simulated UIO-66 MOF (a), FTIR spectra (b).

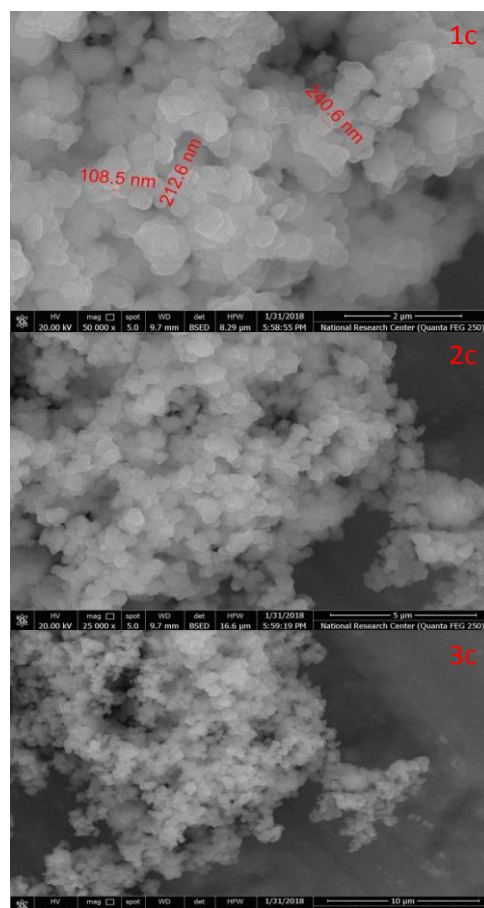


Figure (2): FE SEM of prepared UIO-66 MOF at different magnification scale (1c 2 μm, 2c 5 μm, 3c 10 μm).

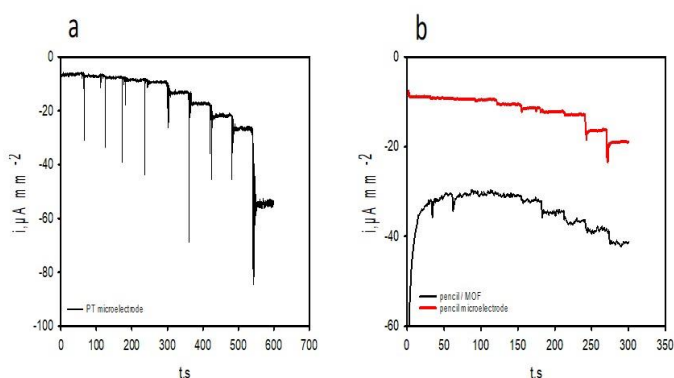


Figure (3): The amperometric response of indicated microelectrodes upon successive injection of  $H_2O_2$  in 50 mM KPP, pH 6.0, at -0.4 V. (a) platinum microelectrode with a diameter of 25 μm, (b) pencil electrode with a diameter of 0.5 mm unmodified and modified with MOF.

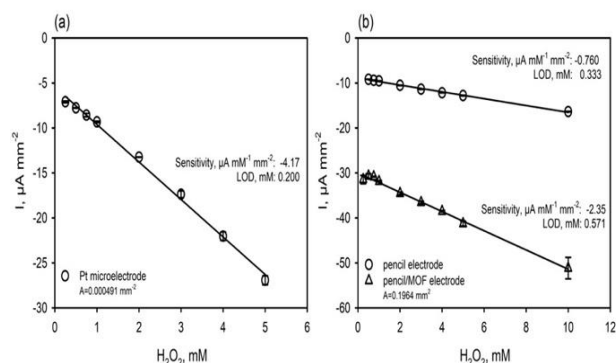


Figure (4): Calibration curves of indicated microelectrodes for hydrogen peroxide detection. (a) platinum microelectrode with a diameter of 25 μm, (b) pencil electrode with a diameter of 0.5 mm unmodified and modified with MOF.

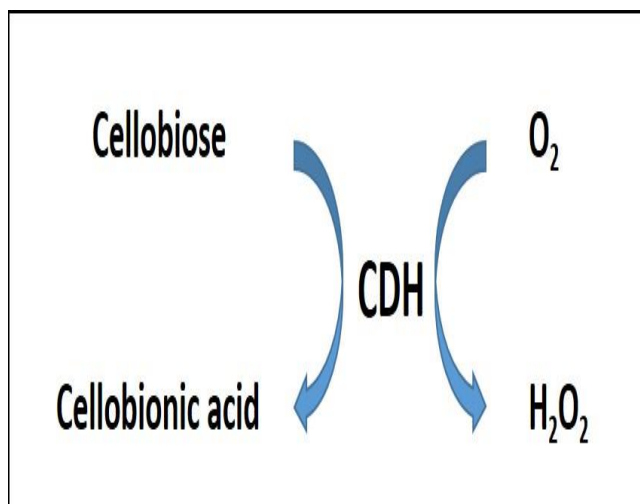


Figure (5): Schematic representation of reactions taking place between pencil electrode and CDH immobilized on surface of cellulose paper in the electrochemical cell.

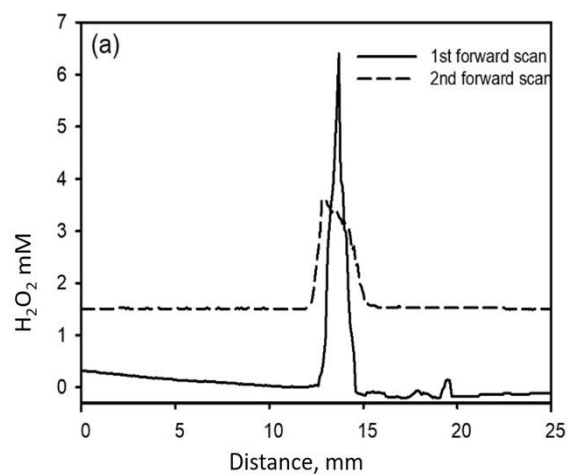


Figure (6): 2D-scanning electrochemical microscopy for detection H<sub>2</sub>O<sub>2</sub> produced by CDH using (a) modified pencil electrode/CDH.

**Table 1** Comparison of the analytical parameters values of MOF modified electrode for hydrogen peroxide detections

Modified electrode	Linear range (mM)	Limit of detection (LOD), [ $\mu$ M]	Sensitivity	Ref <sup>a</sup>
UIO-66/PGE <sup>2</sup>	0.5-20	610	2.16 $\mu$ A mM <sup>-1</sup> mm <sup>-2</sup>	This work
AP-Ni-MOF/CPE <sup>3</sup>	0.004-60	0.9	NP	(Sherino et al. 2018)
AgNPs-Zn- MOF/GCE <sup>4</sup>	0.001-5	0.067	NP	(Arul and John 2017)
Cu-hemin MOFs/CS-rGO	0.00006 – 0.41	0.019	14.5 $\mu$ AM <sup>-1</sup>	(L. Wang et al. 2016)
Pt@UiO-66/GCE	0.005-14.75	3.06	75.33 $\mu$ A mM <sup>-1</sup> cm <sup>-2</sup>	(Xu, Yang, and Xu 2015)
Cu-MOF-MWCNT/ GCE	0.03-0.07	0.46	NP	(Zhou et al. 2014)
Cu-MOF/CPE	0.001–0.9	1.0	NP	(D. Zhang et al. 2015)
Co-MOF/GCE	0.005-9.0	3.76	83.10 A mM <sup>-1</sup> cm <sup>-2</sup>	(Yang et al. 2015)